THE HONG KONG POLYTECHNIC UNIVERSITY

FT BEng (Hons) in ME

Interim Report

Development of an Aerial Air Quality Monitoring Platform Based on Vertical Takeoff and Landing (VTOL) Unmanned Aerial Vehicle (UAV)

by

CHEUNG Hiu Ching, Athena

FUNG Ka Chun, Tim

LIU Sum Yin, Kylie

Supervisor: <u>Prof. WEN Chih Yung</u>

Date of Submission: <u>22 November 2021</u>

Content

1. Nomenclature

α	Angle of attack	m_4	Rear-left motor thrust	ψ	Yaw angle
δ_a	Angular deflection of ailerons	x_b	Front body axis	S	Wing area
δ_e	Angular deflection of elevator	y_b	Right body axis	X	Vehicle state vector
δ_r	Angular deflection of rudder	z_b	Down body axis	u	UAV velocity about x_b axis
δ_{thr}	Forward thrust force	γ_{mot}	p-factor rolling moment coefficient of motor thrust force	v	UAV velocity about y_b axis
L_Q	Arm length for the quadrotor square of UAV	V_a	Magnitude of wind velocity relative to the UAV	w	UAV velocity about z_b axis
c	Chord length	x	North position of UAV	l	UAV moment along x_b axis
C_L	Coefficient of lift	y	East position of UAV		
C_D	Coefficient of drag	z	Down position of UAV	m	UAV moment along y_b axis
C_M	Coefficient of moment	u_P	"Plane" control vector	n	UAV moment along z_b axis
ρ	Density of air	u_Q	"Quad" control vector	p	UAV angular velocity about x_b axis
m_1	Front-right motor thrust	ϕ	Roll angle	q	UAV angular velocity about y_b axis
m_2	Rear-right motor thrust	θ	Pitch angle	r	UAV angular velocity about z_b axis
m_3	Front-left motor thrust				

2. Introduction

2.1. Background

Air pollution monitoring in the Great Bay Aera by a VTOL UAV

The air quality of the Greater Bay Aera can affect millions of people's health. It is important to regulate air quality for the public health concern. Referring to the Innovation and Technology Fund (ITF) project, "Trial: Development of vertical take-off and landing (VTOL) unmanned aerial vehicle (UAV) for air quality monitoring in Greater Bay Area" [1], a traditional method is to send a quadrotor aircraft from a boat at a fixed location to detect the air quality of a limited area alongside the Pearl River. However, this method is time consuming and labor-intensive. Hence, from the ITF project [1], an air quality sensor, which is provided by the Hong Kong Environment Protection Department, aims to be carried by a VTOL UAV to conduct air quality monitoring of the Pearl River Delta Metropolitan Region (PRD).

Airframe selection of the VTOL UAV
Using a fast and long-range VTOL UAV can significantly increase the covered area of each flight. Thus, the efficiency of the monitoring can be greatly improved. Due to the heavy air quality sensor (around 1 kg) and its large size (191mm*79mm*71mm), we would like to choose an airframe with a large fuselage for carrying this bulky payload. Therefore, a swept wing aircraft, Skywalker X8 is chosen. In addition, the quadrotor part is installed at the Skywalker X8 for its VTOL function.

Fig. 1: Our VTOL Skywalker X8 UAV	Fig. 2: Dummy air quality sensor

Reinforcement of the mechanical structure of a VTOL UAV
Since the airframe of the Skywalker X8 is made of polystyrene, we hope to improve its hardness and strength by using composite materials. Also, we would like to redesign the airfoil and remove the winglets because the original design is not suitable for manufacturing the composite wings. Due to its winglets, the difficulties of manufacturing the wings by sticking around four layers of carbon fiber (CF) clothes on a mold increase. Consequently, we would like to choose an airfoil with a flatter design to reduce the complicated steps of manufacturing the composite wings. Besides, assuming the wing-tips vortices can be neglected because of the slow airspeed of our VTOL UAV, we will not design any winglets for our new wings.

2.2. Objectives
The project aims to develop a VTOL UAV for air quality monitoring in Greater Bay Area. This project needs to examine the traditional VTOL aircraft design and the design of the airflow inlet and output of the air quality sensor. Composite materials manufacture technics including mould design, is necessary to enhance the frame of the VTOL UAV. Essential electrical cabling and power system architecture are also required to link the payload and the flight control system. Based on the requirements, the objectives are listed as follows:

i)   *Complete the flight task with the requirements*
        According to the ITF project [1], a VTOL UAV should fly at a speed of 15 to 20 m/s for over 30 minutes and over 30 kilometres with a flight altitude of 100 to 500 metres. The matching lift/drag ratio surpasses 5, and the hover efficiency is within 30 percent of the ideal power loading, and the effective load fraction is no less than 30 percent of the gross weight. In this project, we aimed to flight our VTOL UAV for around 1 hour.

    ii)   *Redesign the wings*

During the project, a more challenging demand is necessary. Although the original Skywalker X8 can already achieve our goals, we would like to enhance the design of the wings to gain better results and simplify its manufacturing process. The Skywalker X8 should accomplish higher flight performance than before after remodelling the design.

    iii)   *Manufacturing fuselage and wings*

To achieve the above requirements and implement the best performances, the good material of the VTOL UAV is essential. The material should be light and hard enough. Therefore, before the structure reinforcement manufacturing progress, a comparison between the materials is needed. We finally decide to build a composited VTOL UAV due to the high stiffness and lightweight of the carbon fibre.

3. Literature Review

3.1. Introduction of Unmanned Aerial Vehicle (UAV)

Remote-control planes and drones are the examples of the unmanned aerial vehicles (UAV). From Hu and Lanzon [2], an UAV generally is a plane that flies without a human pilot, crew, or passengers. Unmanned aerial vehicles (UAVs) are part of an unmanned aircraft system (UAS), which also includes a ground-based controller and a communications system with the UAV. Referring to Cary and Coyne [3], UAV flight can be controlled remotely by a human operator, as in a remotely piloted aircraft (RPA), or with varying degrees of autonomy, such as autopilot help, up to fully autonomous aircraft with no human interaction.

3.2. Introduction of Vertical Take-off and Landing (VTOL)

VTOL is a common technology of UAV. According to Laskowitz[4], an aircraft which can hover, take off, and land vertically is known as a vertical take-off and landing (VTOL) aircraft. Fixed-wing aircraft, as well as helicopters and other aircraft with powered rotors, such as cyclogyros, cyclocopters, and tiltrotors, are all included in this categorization.

3.3. Comparison between different types of UAV

In this comparison, we only focus on the UAVs which can be controlled by a remote controller and the power source of them should be LiPo battery only.

Duration and range

The different structures of UAVs lead to different durations and ranges. Fixed-wing-multi-rotor hybrid UAV (FWR-Hybrid UAV) has both vertical rotors and wings. A study of FWR-Hybrid UAV [5] stated that since FWR-Hybrid UAV has two goals of motors for generating lift and thrust respectively, it has greater power distribution than quadrotor. Hence, it consumes less battery to fly longer and further. However, as it carried more motors, the electricity economy and duration are lower than a fixed-wing UAV which usually just carries one motor. Fig. 3 also shows that the FWR-Hybrid UAV can fly longer than the multi-rotor UAV but slightly shorter than fixed-wing UAV with the same weight, where these results can be estimated by comparing the data of the flight time per kg of each type of UAV [6].
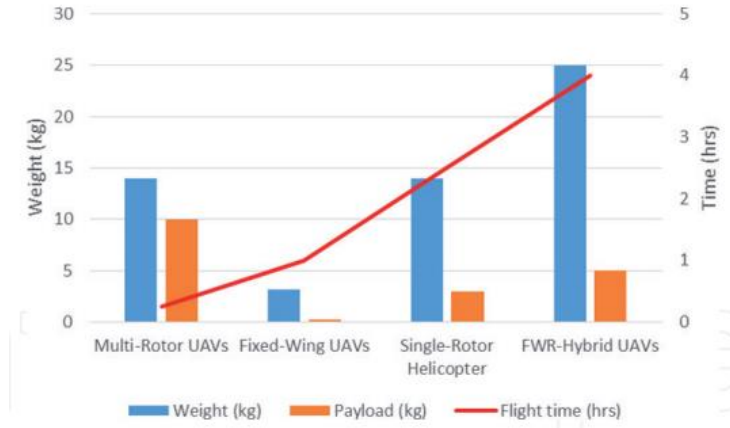
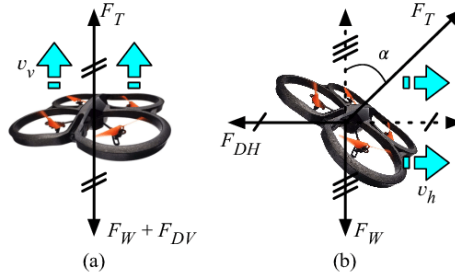Fig. 3: UAV weight and payload vs. flight time [6].

Speed

Fig. 4: Forces on quadcopter in VTOL mode (a) and thrust mode (b) [7]

The speeds of different UAVs can be determined by analyzing their applied forces. For a quadcopter, it has to lean for moving forward because it has only four vertical rotors. In this situation, as explained through the force analysis with the free body diagram in Fig. 4 [7], the thrust of the quadcopter is generated by sharing the lift force. Consequently, the speed of the quadcopter must always be slower than the fixed-wing UAV and FWR-Hybrid UAV the under same power out. Besides, as the fixed-wing UAV has the least aerodynamic drag, it is the fastest.

Abilities

To be versatile, an UAV should have high maneuverability. The existence of lift motors allows quadcopters and FWR-Hybrid UAVs to achieve more motions than fixed-wing UAVs. In the above comparison, FWR-Hybrid UAV has a higher speed and longer duration than a quadcopter. It turns out a result that FWR-Hybrid UAV can be applicable for more tasks. A study of FWR-Hybrid UAV [5] tested itself and a quadcopter to carry out air delivery and water sampling respectively. The results found that the FWR-Hybrid UAV performed better than the quadrotor, especially since the former one flies faster.

Conclusion of the UAVs' comparison

According to the above analyses, FWR-Hybrid UAV combines the advantages of both fixed wing and quadrotor. It can obtain the high maneuverability of quadrotor and the high duration of the fixed wing.
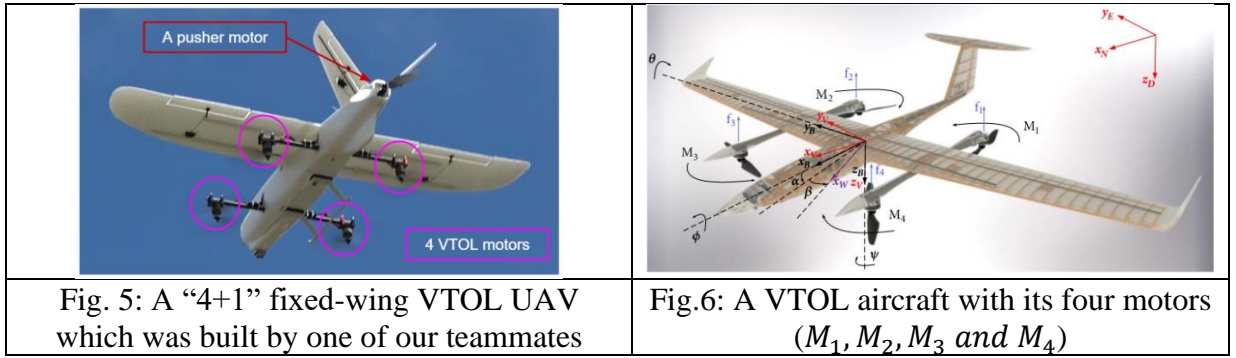
5

	Fixed Wing UAV	FWR-Hybrid UAV	Quadcopter
Flying Mechanism	Take-off and Landing, and Flying: A pair of wings & a pusher rotor	Take-off and Landing: Four rotors besides the fuselage Flying: A pair of wings, a pusher rotor & VTOL part	Take-off and Landing, and Flying: Four rotors as VTOL part
Shape	Streamlined shape	Hybrid of drone and fixed wing UAV	X shape or Plus shape
Type(s) of motors	DC brushless motors & servo motors	DC brushless motors & servo motors	DC brushless motors
Duration	Very High	High	Low
Speed	Very High	High	Low
Maneuverability	Low	High	Very High

Table 1: Comparison of the UAVs

3.4. Aerodynamics and dynamics of fixed-wing VTOL UAV(Athena)

Fig. 5: A "4+1" fixed-wing VTOL UAV which was built by one of our teammates	Fig.6: A VTOL aircraft with its four motors $(M_1, M_2, M_3$ and $M_4)$

A full flight of a fixed-wing VTOL UAV includes its take-off, transition to cruise and landing, and landing. In this project, we would like to focus on "4 +1" fixed-wing VTOL UAV which has four VTOL motors and one pusher motor. An example is show in Fig. 3. According to Mathur and Atkins [8], several equations can present the aerodynamics and dynamics of a fixed-wing VTOL UAV from its take-off to landing. Fig. 4 indicates the axes and angles of a VTOL aircraft. The dynamic equation of the VTOL UAV during its whole flight is shown as follow:

$$\dot{X} = f(X, u_P, u_Q) ,$$

where $X = [x\ y\ z\ u\ v\ w\ \phi\ \theta\ \psi\ p\ q\ r]^T, u_P = [\delta_a\ \delta_e\ \delta_r\ \delta_{thr}]^T, u_Q = [m_1\ m_2\ m_3\ m_4]^T$

During take-off and landing
A fixed-wing VTOL UAV acts as a quadcopter with a pair of fixed-wing when it takes off and lands. Only the 4 VTOL motors will rotate while the pusher motor and all the elevons and ailerons will stop rotation. Hence, the aerodynamics of the VTOL UAV is similar to the one of the quadrotors. Therefore, the wing and tail aerodynamics forces and moments of the VTOL UAV are assumed to be negligible. Also, the airspeed of the VTOL UAV should be low for reducing the aerodynamics surface effects to support the above assumption. The forces and moments acting on the VTOL UAV during its vertical take-off and landing are:

$$\begin{bmatrix} F_x \\ F_y \\ F_z \end{bmatrix} = \begin{bmatrix} 0 \\ 0 \\ -(m_1 + m_2 + m_3 + m_4) \end{bmatrix} \text{ and } \begin{bmatrix} l \\ m \\ n \end{bmatrix} = \begin{bmatrix} \frac{L_Q}{2} * (-m_1 - m_2 + m_3 + m_4) \\ \frac{L_Q}{2} * (m_1 - m_2 - m_3 + m_4) \\ \gamma_{mot} * (m_1 - m_2 + m_3 - m_4) \end{bmatrix},$$

where the p-factor, γ_{mot} should be found experimentally.

During transitions
There are two types of transitions of the fixed-wing VTOL UAV. From Mathur and Atkins [Athena2], the Quad-to-Plane (Q2P) and Plane-to-Quad (P2Q) transitions must be executed for ensuring the VTOL performance and the forward propulsion system of the VTOL UAV can be function well.

For Q2P transition, it aims to provide a smooth transition from hover to the aircraft trim state for the cruise of the VTOL UAV. The velocities of the four VTOL motors will start decreasing while the pusher motor starts its rotation. The four VTOL motors will ramp down to zero when the rotation of the pusher motor remain steady. This can avoid the VTOL UAV suddenly dropping down due to zero thrust and give sufficient time for the VTOL UAV to reach its trim state. Hence, the VTOL UAV can do its cruise mission by its plane mode.

Conversely, for P2Q transition, a smooth transition from the aircraft trim state back to hover for landing should be provided. The tail rotor will start to ramp down and the elevator should pitch up in order to reduce the forward speed of the VTOL UAV. When the airspeed drops below enough, such as 1 m/s, the four VTOL motors can start the rotation and the VTOL UAV will act as a quadcopter to get ready for landing.

During cruise
Unlike during take-off and landing, the fixed-wing VTOL UAV acts as a plane rather than a quadcopter when it is cruising. The tail rotor will provide a forward thrust while some servo motors will control the movements of the ailerons, elevons and rudders. The aerodynamic lift, drag and moment of the VTOL UAV can be calculated at a given angle of attack, α for the wing from the relevant airfoil database with the aerodynamics coefficients.

$$Lift = \frac{1}{2}\rho V_a^2 S C_L; \; Drag = \frac{1}{2}\rho V_a^2 S C_D \text{ and } Moment = \frac{1}{2}\rho V_a^2 c S C_M$$

3.5. Composite wing

Carbon fiber composites are now widely applied in many branches of industries for advanced purposes. They demonstrate high performances to the products by providing a high strength to weight ratio. From the findings of Material Science Research India [9], take the common intermediate modulus (type IM) carbon fiber to compare, the modulus of it is between 200-350 Gpa which is close to that of steel (190-217 Gpa) but at the same time its density (1.76-$1.93 g/cm^3$) is much lower than those of steel (7.75-8.05 g/cm^3). Although the density of IM Carbon Fiber is higher than polystyrene which is the material of Skywalker X8's wings, it is still worth trading off for its strength. The total weight of the hollow carbon fiber wings can also be closer to the solid polystyrene one.

	IM Carbon Fiber	Steel	Polystyrene
Young Modulus	200-350 Gpa	190-217 Gpa	3-3.6 Gpa
Density	1.76-1.93 g/cm^3	7.75-8.05 g/cm^3	0.96-1.05 g/cm^3

Table 2: Tim. Young modulus and densities of IM Carbon Fiber, Steel and Polystyrene [9]

While comparing with another popular composite-fiberglass, carbon fiber is still stiffer. Referring to the test by applying pressure force of 500Pa at the bottom surface of the specific wing at center of pressure using ANSYS Static Structural [10], the total deformation of Epoxy-carbons is both smaller than the epoxy glass. It is also inspiring that carbon fiber composite can allow a higher flexibility on airfoil design because of less concern on the stiffness and weight.

Materials	Total deformation (mm)
Epoxy-carbon UD	4.223
Epoxy S-glass UD	9.8794
Aluminum 2024 T3	6.7377
Epoxy-carbon Woven	7.9845
Epoxy E-glass	10.943

Mode shape	Epoxy-Carbon UD	Epoxy S-Glass	Aluminum 2024 T3	Epoxy-Carbon Woven	Epoxy E-Glass
1	0.84036	0.7176	0.60774	0.84665	0.7172
2	1.38780	0.8117	0.61325	0.85416	0.7855
3	1.10660	1.3689	0.60580	0.84461	1.3456
4	0.79319	0.7027	1.08580	1.50790	0.7043
5	1.63000	0.7843	0.62033	0.85557	0.7491
6	1.61390	1.4494	0.63568	0.90700	1.4152

Fig. 7: wing deformation under pressure	Fig. 8: Tim. Maximum amplitude(mm) of vibration of different materials and wing mode shapes [10]

Epoxy-Carbon UD and Epoxy-Carbon Woven are the two common carbon fiber composites. According to Fig. 8, it can be seen that in most of the wing mode shapes, Epoxy-Carbon Woven has a lower maximum amplitude of vibration than that of Epoxy-Carbon UD and is close to the one of Aluminum 2024 T3. It implies that using this type of carbon fiber composite can help with the UAV's stability and thus less damage to the structure as well as the electronic parts inside.

4. Methodology
4.1. Design flowcharts
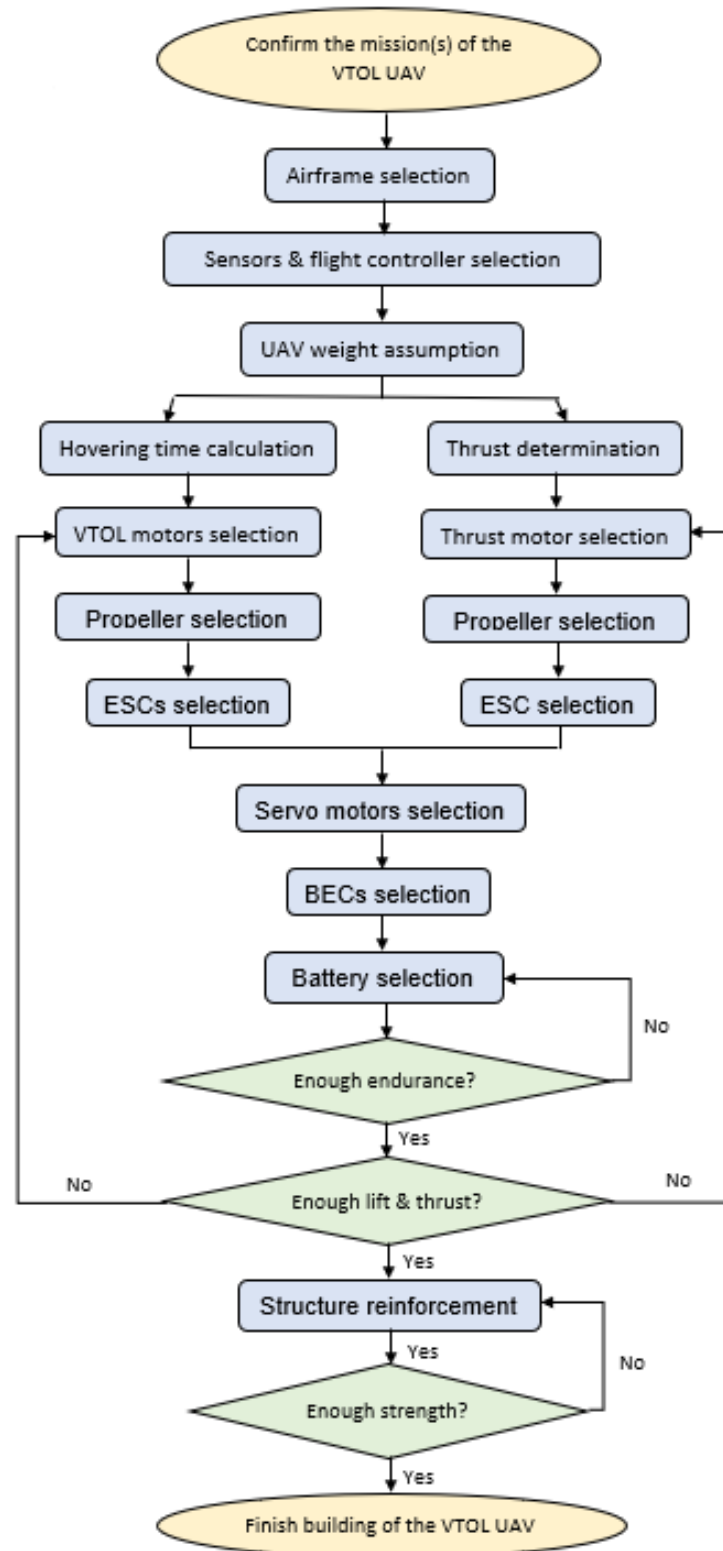### 4.1.1. Design flowchart of building a VTOL UAV

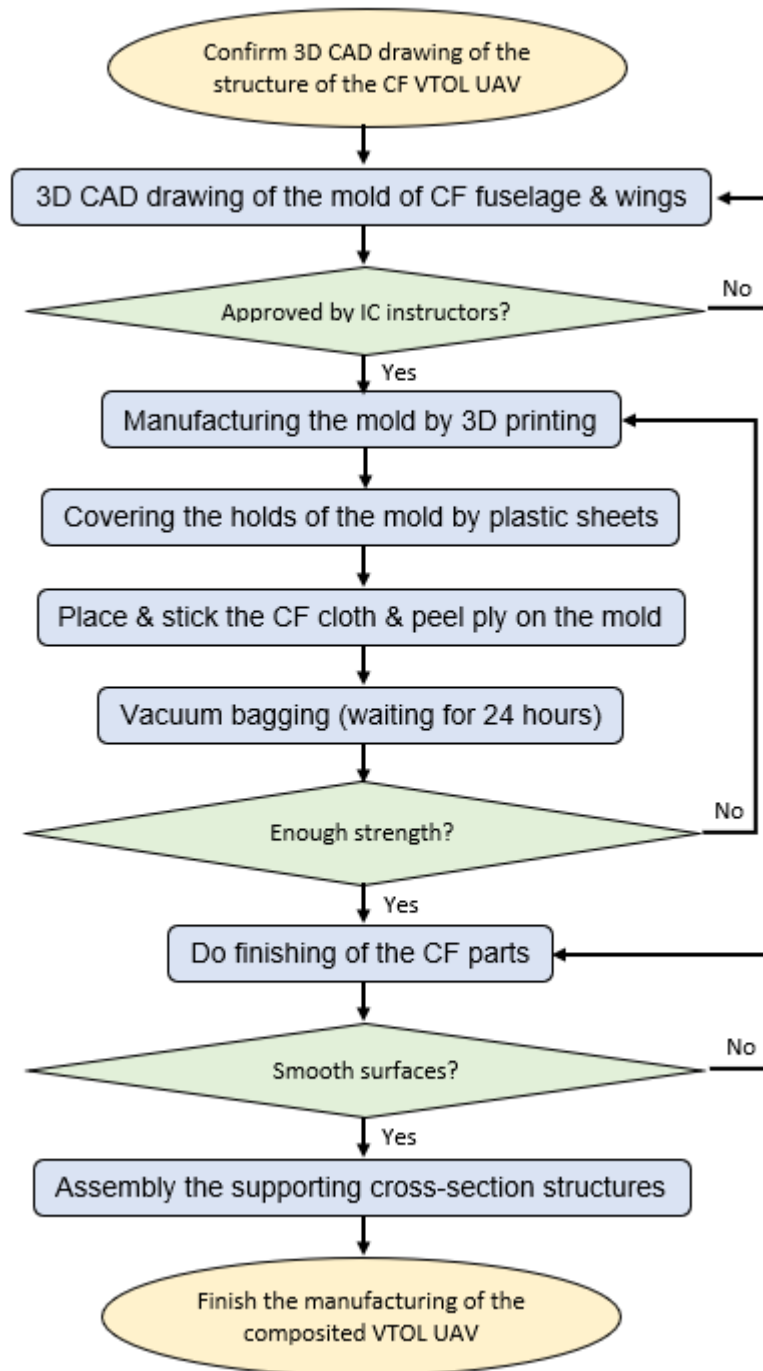Fig. 9: Design flowchart of building a VTOL UAV

Fig. 10: Design flowchart of manufacturing a composited VTOL UAV

4.2. VTOL Skywalker X8 UAV design

Specification of the Skywalker X8

Wingspan	2120 mm	Wing area	0.8 m^2
Fuselage length	790 mm	C.G.	From head to back 430-440 mm

Table 3: Specification of Skywalker X8 [11]

Structure of Skywalker X8

Fig. 11: Structure of Skywalker X8

The main structure of Skywalker X8 can be divided into winglets, wings, and fuselage. There are also two orange plastic connectors which are the linkages between the fuselage and the wings. This design can provide a quick installation or disassembly of the wings so that we can transport the Skywalker X8 by separating its fuselage and wings. This increases its portability.

Take-off Weight Estimation

Item	Weight (g)	Quantity	Total weight (g)
Airframe: Skywalker X8 (Fuselage + wings)	1500	1	1500
Servo motor (EMAX ES3104) & BEC	19.5	2	39
Carbon fiber tube (length: 889mm)	37	1	37
Carbon fiber tube (length: 589mm)	24.9	1	24.9
Carbon fiber tube (length: (956mm)	135	2	270
ESC	20	5	100
Flight controller: Pixhawk 4	33.1	1	33.1
GPS & Gyroscope & Safety switch	35.1	1	35.1
Airspeed sensor (Holybro Digital Air Speed Sensor)	45.4	1	45.4
Radio Telemetry	20	1	20
2.4 GHz Receiver (FrSky TFR8 SB Receiver)	11.4	1	11.4
Wi-Fi Module	5	1	5
Payload (Dummy air quality sensor)	910	1	910
		Total weight (g)	3030.9

Table 4: Take-off Weight Estimation before VTOL motors selection

The weights of the basic electronics such as sensors and flight controllers are measured. The total weight of the Skywalker X8 excluded the VTOL part is assumed and shown in the above table.

Motor Selection

The performances of all motor-propeller combination candidates are processed via the excel with thrust/current data collected from the manufacturers. The assume total weight includes the assumed take-off weight in Table 4, assumed weight of pusher motor, weight of the specific four motors and the four propellers. One example is shown as follow:
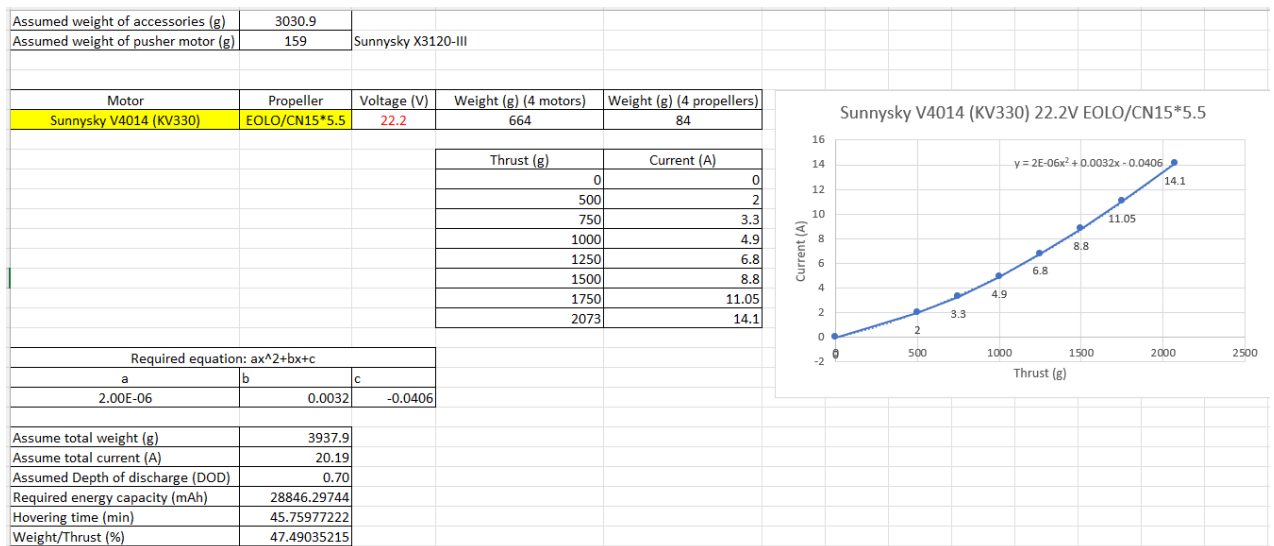
Assumed weight of accessories (g)	3030.9	
Assumed weight of pusher motor (g)	159	Sunnysky X3120-III

Motor	Propeller	Voltage (V)	Weight (g) (4 motors)	Weight (g) (4 propellers)
Sunnysky V4014 (KV330)	EOLO/CN15*5.5	22.2	664	84

Thrust (g)	Current (A)
0	0
500	2
750	3.3
1000	4.9
1250	6.8
1500	8.8
1750	11.05
2073	14.1

Sunnysky V4014 (KV330) 22.2V EOLO/CN15*5.5

$y = 2E\text{-}06x^2 + 0.0032x - 0.0406$

Required equation: ax^2+bx+c		
a	b	c
2.00E-06	0.0032	-0.0406

Assume total weight (g)	3937.9
Assume total current (A)	20.19
Assumed Depth of discharge (DOD)	0.70
Required energy capacity (mAh)	28846.29744
Hovering time (min)	45.75977222
Weight/Thrust (%)	47.49035215

Fig. 12: Motor-propeller performance analysis

And the comparison of the motor-propeller combinations is:

Motor	Propeller	Votage (V)	Weight/Thrust (%)	Hovering time (min)
Sunnysky V4014 (KV330)	EOLO/CN15*5.5	22.2	47.49	45.76
Sunnysky V4014 (KV330)	EOLO/CN15*5.5	25	38.68	59.75
Sunnysky V4014 (KV330)	EOLO CN17*6.2	22.2	35.49	58.25
Sunnysky V4014 (KV330)	EOLO CN17*6.2	25	29.58	62.81
T-motor 4006 (KV380)	T-motor 13*4.4CF	24	53.87	60.55
T-motor 4006 (KV380)	T-motor 14*4.8CF	24	44.79	60.44
T-motor 4006 (KV380)	T-motor 15*5CF	24	40.03	64.56
Tarot 5008 (KV340)	Falcon 1855CF	22.2	34.20	47.33
T-motor MN4014 (KV330)	T-motor 15*5CF	22.2	40.71	52.74
T-motor MN5208 (KV340)	T-motor 15*5CF	24	38.22	49.26
T-motor MN5208 (KV340)	T-motor 16*5.4CF	24	39.41	49.16

Table 5: Comparison of different motor-propeller combinations

Regarding to the hovering time estimation, T-motor 4006 (KV380) with T-motor 15*5CF can provide longest hovering time, 64.56 minutes, so it is selected. Besides, it has an acceptable weight/thrust ratio which is below 50%.

List of Flight Components

Airframe	Skywalker X8
Flight Controller	Pixhawk 4 (Software: AutoPilot)
Power Management Board	Holybro Pixhawk 4 Power Module (PM07)
VTOL Motors	T-motor 4006 (KV380)
VTOL motors' Electronic Speed Controller (ESC)	HobbyWing XRotor 40A
Thrust Motor	Sunnysky X3120-III
Thrust motor's ESC	HobbyWing FlyFun V5 60A
Servo Motors	EMAX ES 3104

Servo Motors' Battery Eliminator Circuit (BEC)	HobbyWing UBEC 5V
Propeller	T-motor 15*5CF
GPS & Gyroscope & Safety Switch	HolyBro Pixhawk 4 Neo-M8N GPS
Airspeed sensor	Holybro Digital Air Speed Sensor
2.4 GHz Receiver	FrSky TFR8 SB Receiver
Power	Grignard Ace Tattoo LiPo Battery 22.2V

Table 6: Accessories of the VTOL Skywalker X8

Assembly of VTOL Skywalker X8

Since we would like to transform the Skywalker X8 to a VTOL UAV, it is necessary to construct the stands for mounting the four rotors. The solution is to add two carbon rods below the wings with a mount on each. Fig. 13 presents the mounts of the VTOL part below.

Fig. 13: Overview of the VTOL part of our VTOL Skywalker X8 UAV	Fig. 14: Electronics wires are inserted into the carbon fiber tubes

To install the four brushless motors as the VTOL motors on the Skywalker X8, two extra carbon tubes are added. As only two carbon rods and the orange plastic connectors above are the original supporting components for mounting the wings, we designed a mounting, which is made by 3D printing, to be the linkage of the carbon rods and the extra carbon tubes. The mounting is stuck under each polystyrene wing by expanded polystyrene glue. Several holes are drilled on the tubes for mounting the VTOL motors and fixing the position of the tubes with the 3D printing mounting. The electronics wires of the motors and their ESC are inserted into the tubes to prevent the broken wires connection due to any accidents during future flights.
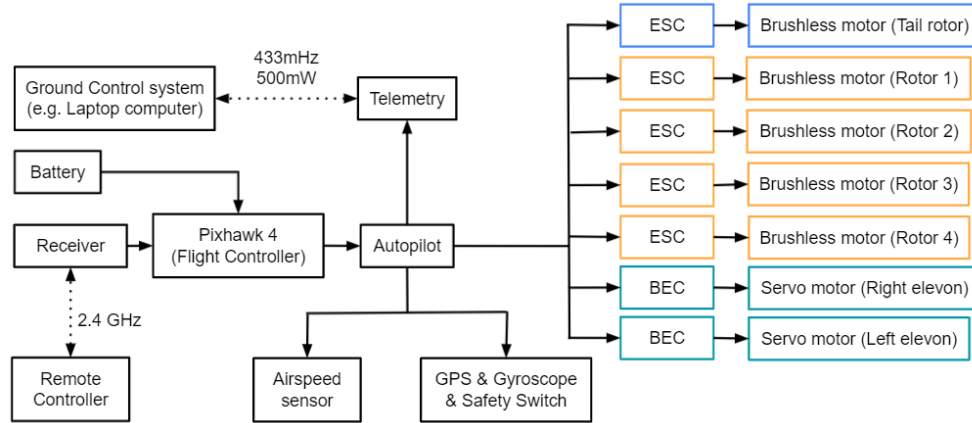
Electronics of VTOL Skywalker X8 UAV

Fig. 15: Connection of the VTOL Skywalker X8 UAV's electronics components

The main concept of the electronics arrangement in Fig. 15 is to connect all the actuators and sensors to the flight controller (Pixhawk 4) so that the controller can process the received signal and control the whole movement of the VTOL Skywalker X8 UAV. The servo motors are supported by the Battery Eliminator Circuit (BEC) while the brushless motors are supported by the electronic speed control (ESC). Apart from these, an airspeed sensor is connected to transfer the collected data back to the ground. Meanwhile, the GPS with gyroscope and safety switch can locate and guide the VTOL UAV by providing the positioning data during flight. A 2.4 GHz remote controller is used to control the VTOL UAV via a receiver. Those sensors and motors work properly under the control of the Pixhawk 4 and its software suite (software: Mission Planner).

For achieving a better management of the external wires of the VTOL part, the wires which inserted into the carbon tube are grouped at each wing. Fig. 16 shows the wires inside a wing. Thus, there are 2 connectors (XT60 and MT30) expose from each wing. At each wing, all the positive and ground wires of the actuators' ESC or BEC are connected by a XT60 connector, while all the signal wires of the actuators are connected by a MT30 connector. Both connectors link to a power management board in Fig. 17. This board can connect the battery and the actuators with Pixhawk 4 for managing the order of the wires and indicating the usage of the wires clearly. Therefore, even wires of the wings' actuators can be connected easily during the assembly by plugging only 4 connectors in total.
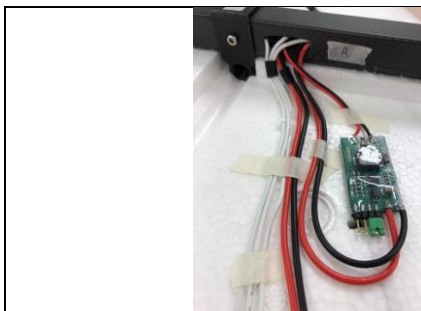

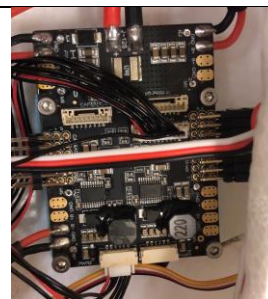| Fig. 16: Electronic wires management inside a wing	Fig. 17: Power Management board in VTOL Skywalker X8 UAV

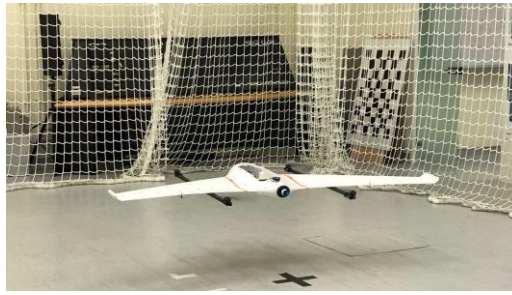*Indoor flight test & preflight checking*

Fig. 18: Indoor hovering test of VTOL Skywalker X8

Before flying the VTOL Skywalker X8 in the outdoor flying field, an indoor hovering test should be induced to ensure the flight performance of the VTOL UAV is stable. The rotating direction of each actuator should be checked to ensure the performance of the VTOL UAV for safety concern. Moreover, the abilities of the sensors should be confirmed before flying the VTOL UAV too. The hovering test of our VTOL UAV is shown in Fig. 18.

4.3. <u>3D scanning of Skywalker X8</u>

The CAD drawing of the Skywalker X8 was created by 3D scanning. The purposes of scanning the Skywalker X8 into a digital file are because some calculations and simulations of the Skywalker X8 are needed to enhance its VTOL design for better performances. Since the Skywalker X8 is quite large which cannot be 3D scanned automatically, we would like to use a portable optical measuring device, handySCAN to do the 3D scanning (Fig. 19). After the 3D scanning, some aftereffects are required to clean up the noise of the scanned files of the object into a full 3D model. Then, some sketches are added to convert the cross-section entities. Finally, exports the CAD drawing to SolidWorks for building the 3D CAD drawing. The details of the 3D scanning are listed in the following:

Fig. 19: Using handySCAN to do the 3D scanning

Scanning the Skywalker X8 by using Vxelements

A software named Vxelements is used to help scan the Skywalker X8. The handySCAN is a moveable scanner that can be moved around all the angles by using hands. The limitation is that some dot labels needed to be stuck on a plane or the Skywalker X8 to be the references point to outline the structures of the UAV. To complete a whole 3D structure of the UAV, different angles are needed to scan. The different scanning angles should be at least three points in triangle shape overlapping with other angles to be the references points for merging.

Editing the scanned files and merge the results

After scanning all the parts and angles, Geomagic Design X should be used to edit the scanned file and merge the different views into a 3D part. First, the scanned files usually got lots of noise. Those noise needed to be deleted and some of the erroneous draft.
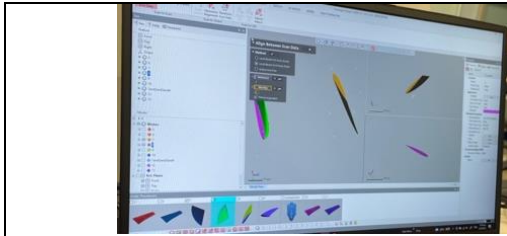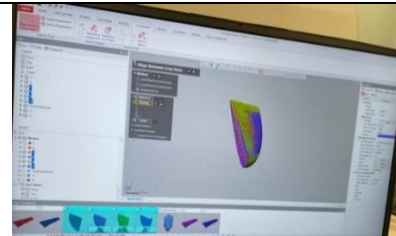

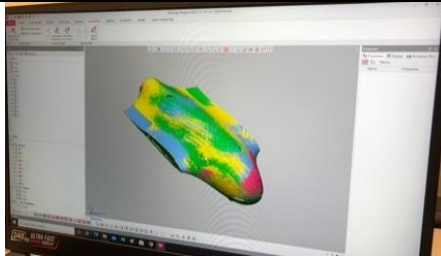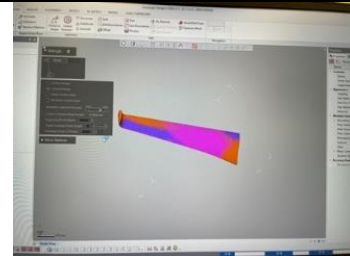|	
Fig. 20: Progress while aligning the wing	Fig. 21: Results after aligning the wing
Fig. 22: Results after aligning the fuselage	Fig. 23: Results after aligning the wing

To merge different views of the parts into a 3D part, a function called align in Design X is needed. First, select the three points mentioned above, which help to be the references points. Both views should be selected with the same point. After aligning the different views, the results should be shown like in Fig. 21. The colour should be evenly distributed. During scanning the Skywalker X8, at least four views of a part are being scanned. Fig. 22 and Fig. 23 show the results after aligning the fuselage and the wing. Both colours are evenly distributed. After aligning all the parts, 'merge' is needed to group all the views into parts.

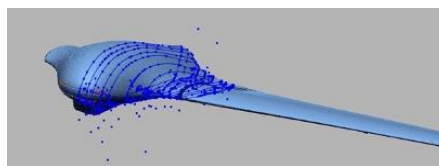*Convent entities from the cross-sections and build the 3D CAD files*

Fig. 24: Conventing the cross-section into entities

Some reference entities need to be converted before exporting the files to SolidWorks for further sketching. Several entities in Fig. 24 have been transformed into references. Every 15 to 30 cm, a reference is placed. The noise in the entities should be removed after exporting them to SolidWorks, and the entities should be smoothed out. The entities converted in Design X are not smooth enough, and some noise may be converted, affecting the entity completeness. Fig. 25 to Fig. 27 show the results. The 3D parts can start building utilizing the loft surface after altering the entity designs and turning them solid. These represent in Fig. 28 to Fig. 30.

Fig. 25	Fig. 26	Fig. 27
Fig. 28	Fig. 29	Fig. 30
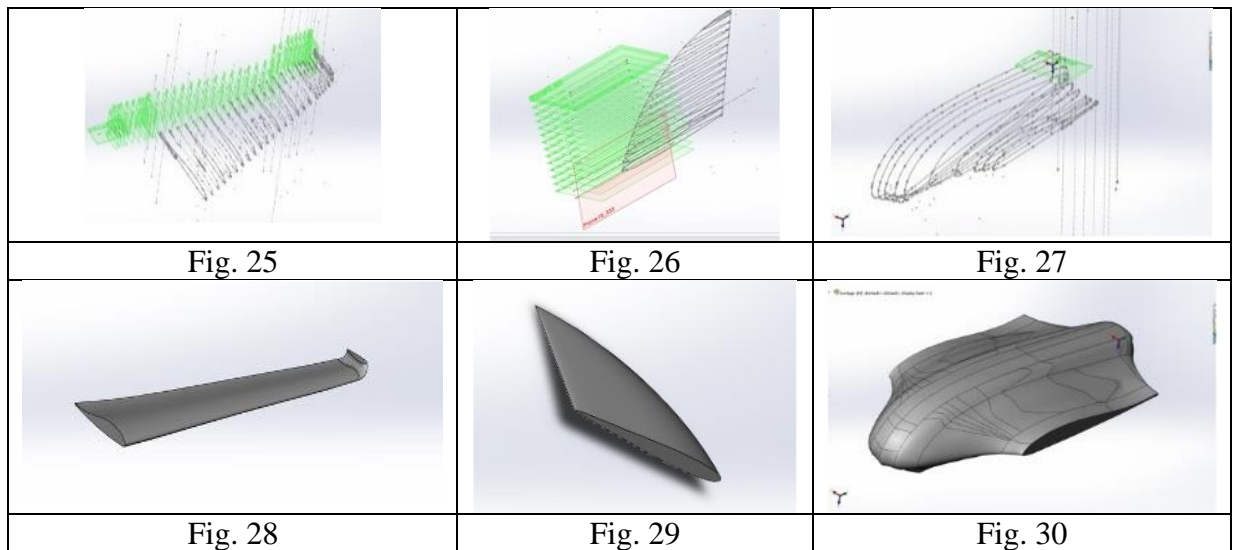
4.4. Calculation and simulation in computational fluid dynamics (CFD)

Comparison between the result of CFD and the flight log

We will apply CFD by using the above 3D CAD drawings to do some calculations on the aerodynamics of the Skywalker X8. We believe that the comparison between our VTOL UAV's flight log and the results in CFD can show us whether the flight performance of the VTOL UAV can reach our expectations or not. Fig. 31 to Fig. 33 are the examples of the graphical analyses in flight logs. Also, it can be a reference for us to design our composited VTOL UAV at the next stage.

Fig. 31	Fig. 32	Fig. 33
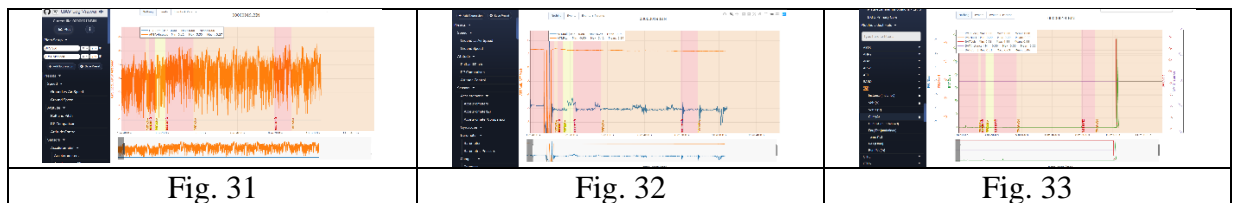
Simulation with our new wings design and comparison with its flight log

Similarly, we will simulate the performance of the composited VTOL UAV by CFD to ensure its 3D CAD drawing design is applicable for this monitoring mission. It can prevent spending extra time to revise the airfoil and repeat the manufacturing steps. Next, we can also compare the simulation results with the flight log of the flight controller to check whether its outdoor flight performance can be satisfied or not.

4.5. Reason of selecting Clark Y airfoil

Better aerodynamics performance

In the aerodynamics aspect, we would like to choose an airfoil with higher C_L/C_D ratio and C_L/α ratio for assuring better flying performance of our composited VTOL UAV. Referring to Gryte et al. [12], the relevant graphs of the data are shown in Fig. 34 to Fig. 35. Regarding the data of Clark Y airfoil, the Airfoil Tools [13] indicated them in Fig. 36 to Fig. 37. As Clark Y airfoil can have higher C_L/C_D ratio and C_L/α ratio than Skywalker X8's, we selected this airfoil for our composited VTOL UAV.
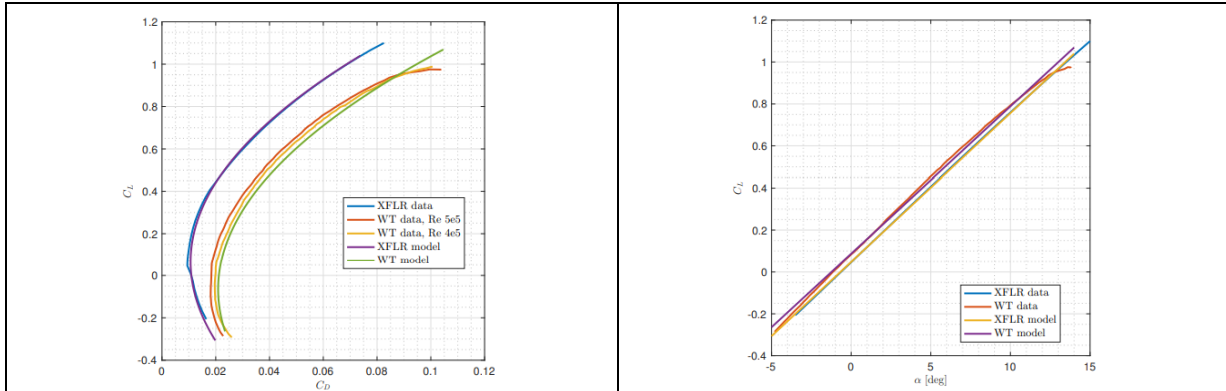
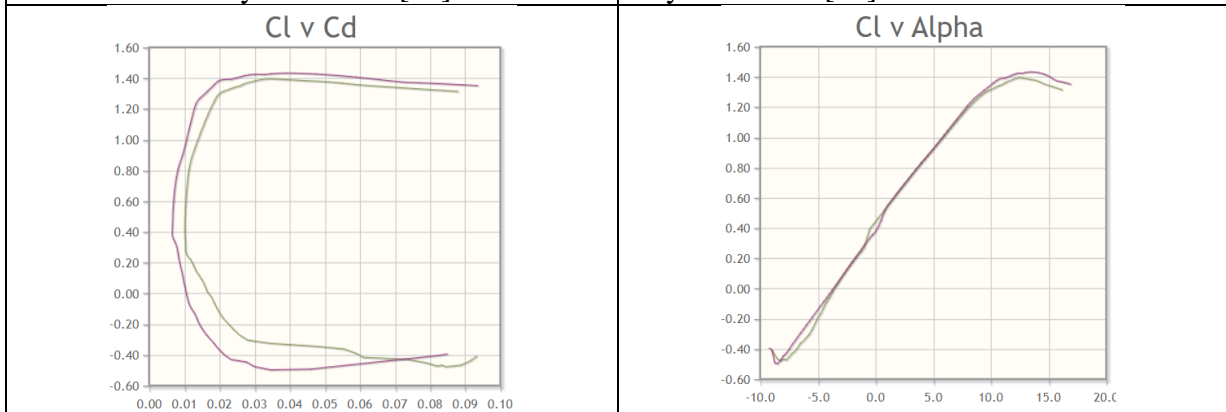|	
Fig. 34: Lift coefficient vs. drag coefficient of Skywalker X8 [12]	Fig. 35: Lift coefficient vs. angle-of-attack of Skywalker X8 [12]
Fig. 36: Lift coefficient vs. drag coefficient of Clark Y airfoil [13]	Fig. 37: Lift coefficient vs. angle-of-attack of Clark Y airfoil [13]

Low flat surface

In the manufacturing aspect, the difficulty of demolding a composited curved surfaces part is much greater than the one of a composited flat surfaces part. Therefore, we would like to choose Clark Y airfoil due to its flat lower surface. Fig [Athena 3] shows the shape of the Clark Y airfoil.
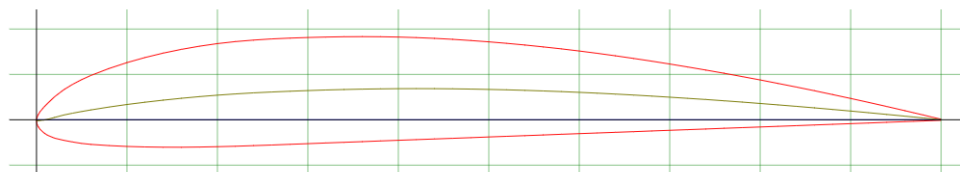

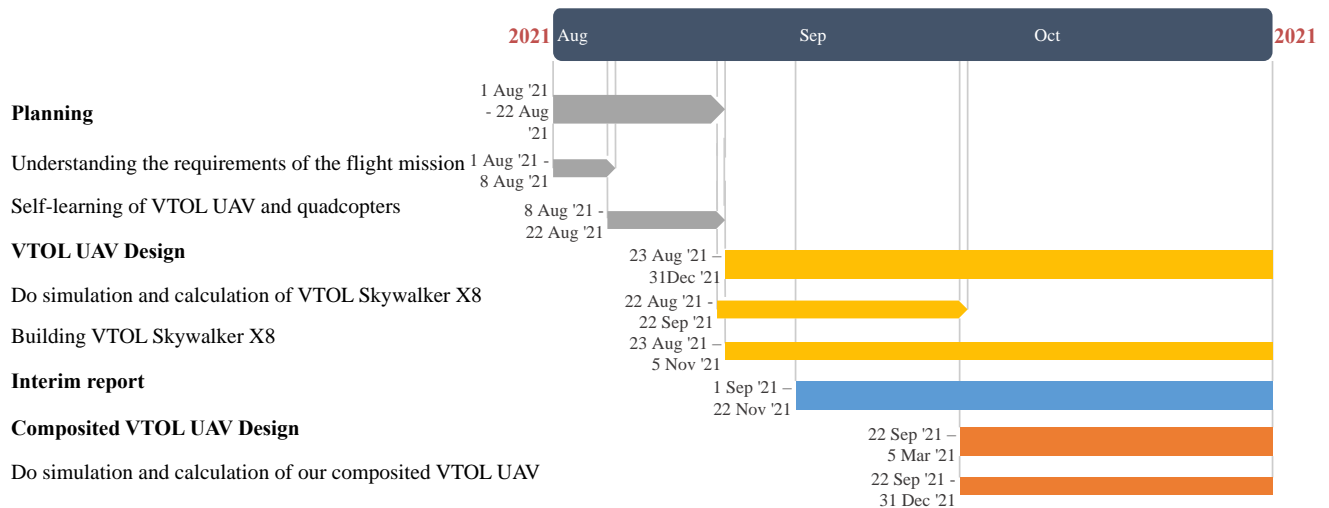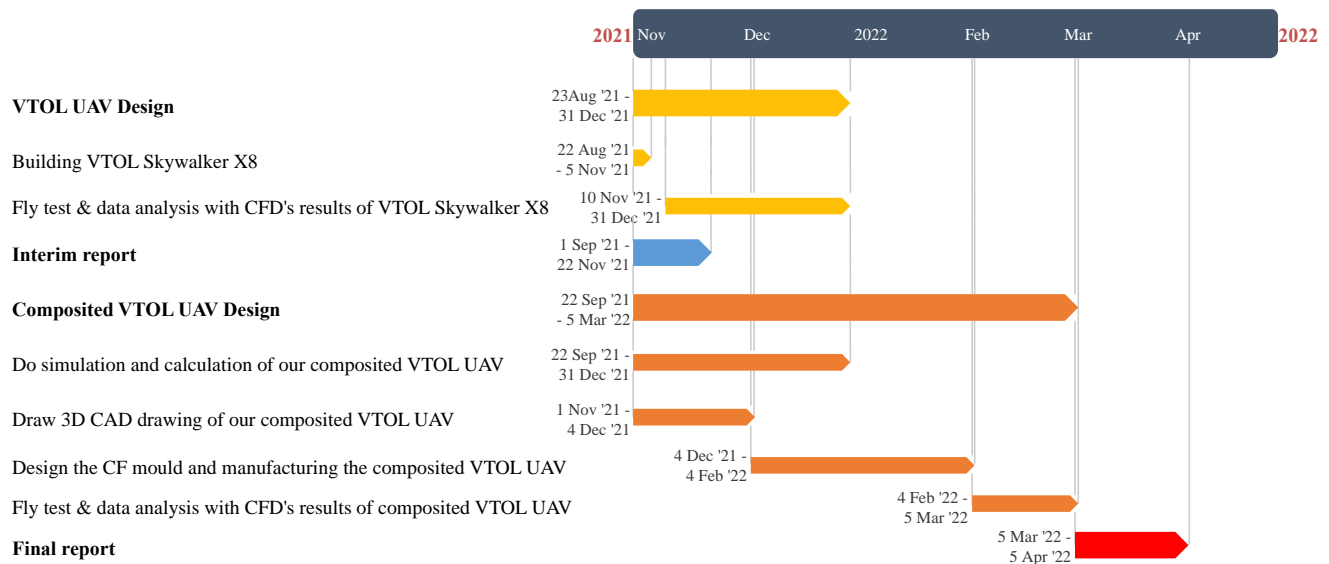Fig. 38: Shape of Clark Y airfoil [13]

5. Project Planning

5.1. Project Schedule

Description	Start date	End date	Duration (days)
Planning	01/08/2021	22/08/2021	22
Understanding the requirements of the flight mission	01/08/2021	01/08/2021	1
Self-learning of VTOL UAV and quadcopters	08/08/2021	22/08/2021	15
VTOL UAV Design	23/08/2021	31/12/2021	131
Do simulation and calculation of VTOL Skywalker X8	22/08/2021	22/09/2021	32
Building VTOL Skywalker X8	23/08/2021	05/11/2021	75
Fly test & data analysis with CFD's results of VTOL Skywalker X8	10/11/2021	31/12/2021	52
Interim report	01/09/2021	22/11/2021	83
Composited VTOL UAV Design	22/09/2021	05/03/2022	165
Do simulation and calculation of our composited VTOL UAV	22/09/2021	31/12/2021	101
Draw 3D CAD drawing of our composited VTOL UAV	01/11/2021	04/12/2021	34
Design the CF mold and manufacturing the composited VTOL UAV	04/12/2021	04/02/2022	63
Fly test & data analysis with CFD's results of composited VTOL UAV	04/02/2022	05/03/2022	30
Final report	05/03/2022	05/04/2022	32

Table 7: Schedule of this project

5.2. Gantt Chart

VTOL UAV Design — 23Aug '21 - 31 Dec '21

Building VTOL Skywalker X8 — 22 Aug '21 - 5 Nov '21

Fly test & data analysis with CFD's results of VTOL Skywalker X8 — 10 Nov '21 - 31 Dec '21

Interim report — 1 Sep '21 - 22 Nov '21

Composited VTOL UAV Design — 22 Sep '21 - 5 Mar '22

Do simulation and calculation of our composited VTOL UAV — 22 Sep '21 - 31 Dec '21

Draw 3D CAD drawing of our composited VTOL UAV — 1 Nov '21 - 4 Dec '21

Design the CF mould and manufacturing the composited VTOL UAV — 4 Dec '21 - 4 Feb '22

Fly test & data analysis with CFD's results of composited VTOL UAV — 4 Feb '22 - 5 Mar '22

Final report — 5 Mar '22 - 5 Apr '22

6. **References**

[1] "Trial: Development of vertical take-off and landing (VTOL) unmanned aerial vehicle (UAV) for air quality monitoring in Greater Bay Area," *Innovation and Technology Fund Public Sector Trial Scheme*

[2] J. Hu and A. Lanzon, "An innovative tri-rotor drone and associated distributed aerial drone swarm control," *Robotics and autonomous systems,* vol. 103, pp. 162-174, 2018, doi: 10.1016/j.robot.2018.02.019.

[3] L. Cary and J. Coyne, "ICAO Unmanned Aircraft Systems (UAS), Circular 328," *UVS International, Blyenburgh & Co,* vol. 2012, pp. 112-115, 2011.

[4] I. B. Laskowitz, "Vertical take-off and landing (VTOL) rotorless aircraft with inherent stability," *Annals of the New York Academy of Sciences,* vol. 93, no. 1, pp. 3-24, 1961.

[5] Aseem Saini and Mukul Chhabra, "Hybrid VTOL-UAV for Air Delivery and Sampling Purposes", B.Tech dissertation, Dept. Elect & Com. Eng., Indraprastha Institute of Information Technology,. New Delhi, 2018.

[6] Chika Yinka-Banjo and Olasupo Ajayi, "Sky-Farmers: Applications of Unmanned Aerial Vehicles (UAV) in Agriculture," IntechOpen, 2019.

[7] D. Baek, Y. Chen, A. Bocca, A. Macii, E. Macii, and M. Poncino, "Battery-Aware Energy Model of Drone Delivery Tasks," in Proceedings of the International Symposium on low power electronics and design, 2018, pp. 1–6, doi: 10.1145/3218603.3218614.

[8] A. Mathur, E. M. Atkins, "Design, Modeling and Hybrid Control of a QuadPlane", presented at AIAA Scitech 2021 Forum. [Online]. Available: https://www.researchgate.net/publication/348254161_Design_Modeling_and_Hybrid_Control_of_a_QuadPlane [Accessed Nov. 20, 2021].

[9] Bhatt, & Goe, A. (2017). Carbon Fibres: Production, Properties and Potential Use. Material Science Research India, 14(1), 52–57. https://doi.org/10.13005/msri/140109 [Accessed Nov. 15, 2021].

[10] S. Kumar Das and S. Roy, "Finite element analysis of aircraft wing using carbon fiber reinforced polymer and glass fiber reinforced polymer," IOP conference series. Materials Science and Engineering, vol. 402, no. 1, p. 12077, 2018, doi: 10.1088/1757-899X/402/1/012077.

[11] Skywalker X8. [Online]. Available: http://skywalkermodel.com/en/76.html [Accessed Nov 20, 2021].

[12] K. Gryte, R. Hann, M. Alam, J. Rohac, T. A. Johansen, and T. I. Fossen, "Aerodynamic modeling of the Skywalker X8 Fixed-Wing Unmanned Aerial Vehicle," presented at 2018 International Conference on Unmanned Aircraft Systems (ICUAS). [Online]. Available: https://www.researchgate.net/publication/327517108_Aerodynamic_modeling_of_the_Skywalker_X8_Fixed-Wing_Unmanned_Aerial_Vehicle [Accessed Nov. 20, 2021].

[13] Airfoil Tool, "CLARK Y AIRFOIL (clarky-il)," [Online]. Available: http://airfoiltools.com/airfoil/details?airfoil=clarky-il#polars [Accessed Nov 20, 2021].